Wood modification by furfuryl alcohol caused delayed decomposition response in *Rhodonia (Postia) placenta*

Postia placenta; wood decay; wood modification; wood protection; furfurylation; gene regulation; transcriptome; radiata pine; *Pinus radiata*

Inger Skrede[1], Monica Hongrø Solbakken[1], Jaqueline Hess[1], Carl Gunnar Fossdal[2], Olav Hegnar[3,4], Gry Alfredsen[4]

[1]Department of Biosciences, University of Oslo, PO Box 1066, NO-0316 Oslo, Norway

[2]Department of Forest Health, Norwegian Institute of Bioeconomy Research, PO Box 115, NO-1431, Ås, Norway

[3]Faculty of Chemistry, Biotechnology & Food Science, Norwegian University of Life Sciences, PO Box 5003, NO-1432, Ås, Norway

[4]Department of Wood Technology, Norwegian Institute of Bioeconomy Research, PO Box 115, NO-1431, Ås, Norway

ABSTRACT

The aim of this study was to investigate differential expression profiles of the brown rot fungus *Rhodonia placenta* (previously *Postia placenta*) harvested at several time points when grown on *Pinus radiata* (radiata pine) and *P. radiata* with three different levels of modification by furfuryl alcohol, an environmentally benign commercial wood protection system. For the first time the entire gene expression pattern of a decay fungus is followed in untreated and modified wood from initial to advanced stages of decay. Results support the current model of a two-step decay mechanism, with an initial oxidative depolymerization followed by hydrolysis of cell-wall polysaccharides. The wood decay process is finished, and the fungus goes into starvation mode after five weeks when grown on unmodified *P. radiata* wood. The pattern of repression of oxidative processes and oxalate synthesis found in *P. radiata* at later stages of decay is not mirrored for the high furfurylation treatment. The high treatment level provided a more unpredictable expression pattern throughout the entire incubation period. Furfurylation does not seem to directly influence the expression of core plant cell wall hydrolyzing enzymes, as a delayed and prolonged, but similar pattern was observed in the *P. radiata* and the modified experiments. This indicates that the fungus starts a common decay process in the modified wood, but proceeds at a slower pace as access to the plant cell wall polysaccharides is restricted. This is further supported by the downregulation of hydrolytic enzymes for the high treatment level at the last harvest point (mass loss 14%). Moreover, the mass loss does not increase the last weeks. Collectively, this indicates a potential threshold for lower mass loss for highly modified wood.

IMPORTANCE

Fungi are important decomposers of woody biomass in natural habitats. Investigation of the mechanisms employed by decay fungi in their attempt to degrade wood is important for both the basic scientific understanding of ecology and carbon cycling in nature, and for applied uses of woody materials. For wooden building materials long service life and carbon storage is essential, but decay fungi are responsible for massive losses of wood in service. Thus, optimizing durable wood products for the future are of major importance. In this study we have investigated the fungal genetic response to furfurylated wood, a commercial environmentally benign wood modification approach, that improves service life of wood in outdoor applications. Our results show that there is a delayed wood decay by the fungus as a response to furfurylated wood and new knowledge about the mechanisms behind the delay is provided.

INTRODUCTION

Wood as a building material has a number of attractive properties including carbon sequestration during its service life and its aesthetic aspects as a natural material. One of the main challenges with using wood as a building material is its susceptibility to attack by wood degrading microorganisms. Traditional wood preservatives with a biocidal mode of action (e.g. organic- or copper-based preservatives) cause concerns due to their perceived negative environmental impacts. In Europe the Construction Products Regulation and the Biocidal Products Regulation have a major impact on the wood industry and the number of active ingredients allowed for wood preservatives is decreasing (1). This, together with new consumer awareness and demand for more environmentally focused products (2), pushes the need for new products and wood protection approaches.

The modern wood modification approach, in contrast to more traditional wood preservatives, is to modify the wood matrix so that it can no longer act as a suitable substrate for wood degrading organisms. Different wood modification approaches were described in detail by Hill (3). Currently the processes underlying available wood modification products can be classified as chemical processing (acetylation, furfurylation, resin impregnation etc.), thermo-hydro processing (thermal treatment) and thermo-hydro-mechanical processing (surface densification) (2). The different wood modification processes are at various stages of development, and the most established processes on the marked include thermal treatment, acetylation and furfurylation.

The commercial wood modification process furfurylation, use furfuryl alcohol which is manufactured industrially by catalytic reduction of furfural obtained from agricultural waste such as sugar cane bagasse or corn cobs (4). It involves a wood impregnation step with furfuryl alcohol

and catalysts, followed by a curing step where the furfuryl alcohol is polymerized within the wood cell walls (2, 4). This is a complex chemical reaction and there is still some discussion whether the furfurylation process only bulks the wood cell wall or if it also causes chemical modifications of the native wood cell wall polymers. As support for the latter theory it has been shown in a model lignin system that the furfural polymer formed covalent bonds with lignin (5). In addition to this uncertainty, the mechanisms utilized by decay fungi in their attempt to degrade modified wood are not well understood at the molecular level and this hinders knowledge-based design of the modification methods.

Independent of how the furfurylation modifies the wood, the process results in improved resistance to fungal deterioration (2-4, 6, 7). The level of modification by furfural alcohol is measured by the Weight Percent Gain (WPG) of the wood. Lande et al. (6) concludes that furfurylated wood treated to a WPG of 35% or more, has sufficient resistance to brown and white rot decay fungi.

Traditionally wood degrading basidiomycetes have been divided into white- or brown rot fungi due to the ability of white rot fungi only to degrade lignin along with holocellulose, while brown rot fungi leave the lignin behind as a brown residue. White rot fungi have a larger repertoire of known enzymes that depolymerize the components of the plant cell wall than brown rot fungi (8). It is important to note that this traditional dichotomy is polyphyletic and it has been suggested, based on comparative studies of 33 basidiomycetes, that a continuum exists, without a clear distinction between the types of decay (8). Brown rot fungi dominate decomposition of conifer wood in boreal forests even if only 6% of fungal wood decay species produce the classical brown rot decay (9). Moreover, brown rot causes more challenges than white rot for wood in service outdoors (10). Brown rot fungi depolymerize cellulose rapidly during incipient stages of wood

97 colonization, resulting in considerable losses in strength even at early decay stages (11, 12). The
98 current hypothesis is that brown rot fungi utilize a non-enzymatic system that rapidly
99 depolymerizes cell wall components in early stages of decay, prior to depolymerization by
100 traditional cellulases and hemicellulases (13-15). This system is often referred to as the Chelator
101 Mediated Fenton (CMF) system and involves the solubilization of iron from the environment by
102 oxalic acid that the fungus secretes, followed by the reduction of iron by chelating/reducing
103 secondary metabolites that then can react with hydrogen peroxide within the wood cell wall. It is
104 theorized that this produces oxygen radicals through a Fenton-like reaction that will depolymerize
105 lignocellulose and make these polymers available for large hydrolytic enzymes (16). This two-step
106 theory has been further supported by the gene expression pattern in *Rhodonia placenta* (17).
107 Whether the CMF functions as a pretreatment of the wood opening the cell walls to allow the
108 enzymes to enter the cell wall, or whether polysaccharide components diffuse into the cell lumen
109 to the enzymes is currently debated (18). However, there is agreement in that the brown rot CMF
110 systems and the hydrolytic enzymes cannot be present at the same time since highly reactive ROS
111 (reactive oxygen species) reactions will cause oxidative damage on glycoside hydrolases. Zhang
112 and Schilling (19) found that cellobiose appears to play a key role in the transition between the
113 oxidative phase and the hydrolytic phase. However, the full extent of feedback mechanisms
114 regulating brown rot decay is not known.

115 *Rhodonia* (*Postia*) *placenta* is a commonly used brown rot decay fungus in laboratory wood
116 decay tests, strain FPRL 280 is included the European standard EN 113 (20) and strain ATCC11538
117 is included in the American standard E10-16 (21). The *R. placenta* strain MAD 698-R, and its
118 monokaryotic strain MAD698-R-SB12 has been genome sequenced by the Department of Energy,
119 Joint Genome Institute (JGI), USA (22, 23). The species has frequently been used as a model

120 fungus for gene expression studies of untreated wood (17, 19, 23-25) and modified wood (26-32),
121 including furfurylated wood (28, 31). These experiments have shown that several hemicellulases
122 but few potential cellulases were produced when the fungus was grown on ball-milled aspen or
123 glucose as substrate (24). The expression patterns for oxidoreductase encoding genes support an
124 extracellular Fenton system. Furthermore, Skyba et al. (33) demonstrated that the gene expression
125 profile of *R. placenta* (and *Phanerochaete chrysosporium*) was influenced by wood substrate
126 composition (three *Populus trichocarpa* genotypes) and the duration of incubation. For early stages
127 of modified wood, a possible shift toward increased expression of genes related to oxidative
128 metabolism and concomitant reduction of several gene products related to the breakdown of
129 holocellulose in furfurylated wood compared to unmodified wood has been suggested (28).

130 In this study we investigated the differential expression profiles of the brown rot fungus
131 *Rhodonia placenta* harvested at several time points when grown on *Pinus radiata* with three
132 different levels of furfurylation. For comparison we also investigated the gene expression during
133 decay of unmodified *P. radiata*. The overall aim is to understand the mechanisms utilized by brown
134 rot decay fungi in their attempt to degrade modified and unmodified wood. This is important for
135 further optimization of future modified wood products, and for an expanded understanding of the
136 fungal decay process in general.

137

RESULTS

In the following experiments the *P. radiata* wood was modified at three different levels. The three modification levels had a mean Weight Percent Gain (WPG) of 3.8±0.7%, 24.0±3.5%, 36.6±5.0%. For simplicity the treatments are named WPG4, WPG24 and WPG37, respectively. The experiment on the unmodified wood is named *P. radiata*.

Mass loss calculations. Five weeks after inoculation of *R. placenta* strain FPRL 280 on the *P. radiata* wood blocks, they had a mean mass + treatment loss of 28.8±4.0%, while the modified WPG37 only had a mean mass + treatment loss of 13.5±3.3% after 21 weeks (Fig. 1). Mass loss is within the wood protection literature mostly referred to as the mass loss of the entire wood + treatment system, i.e. dry weight of the treated wood before fungal inoculation compared to dry weight after fungal decay. Another way to measure mass loss is to assume that only the wood is decayed and eliminate the WPG of the treatment from the mass loss calculation. Both methods resulted in the same general trends, but the exclusion of WPG results in slightly higher mass losses as expected (Fig. S1). The differences between the two mass loss calculation approaches for the three furfurylation levels at the last harvesting points were (wood + treatments vs. only wood): WPG4 week 9 41.7% vs. 42.5%, WPG24 week 21 29.0% vs. 34.6%, WPG37 week 21 13.5% vs. 16.0%. We use the wood + treatment results as presented in Fig. 1 as our mass loss detection system.

Differential gene expression. In order to investigate the genetic basis of the different behavior of *R. placenta* growing on different levels of furfurylated wood we sequenced transcriptomes of a selection of time series using Illumina Nextseq sequencing. The sequenced time points for each treatment were sampled according to the following setup: *P. radiata* – weeks

1, 2, 3, 4 and 5, WPG4 – weeks 3, 6 and 9, WPG24 – weeks 3, 6, 9, 12, 15, and 18, WPG37 – weeks 3, 6, 9, 12, 15 and 18.

Even if the genome and transcriptome of the American *R. placenta* strain MAD 698-R has been sequenced, this could not be used for mapping purposes in this study. The genome sequenced American strain MAD 698-R and the European strain FPRL 280 used in this study are significantly different, with a mapping success of only 40-60% when the reads were mapped to the genome of MAD 698-R (results not shown). We therefore produced Illumina Hiseq paired-end data to be used for a transcriptome assembly. The resulting assembly had 56 520 contigs (transcripts), and covered 99.3% of the conserved BUSCO fungal genes (Table S1; Table S2). In the transcriptome, 9 355 contigs had an annotation from Blastx, and 18 917 contigs were given a PFAM annotation. In all further analyses the sequence data were mapped to this annotated transcriptome assembly. The mapping success of sequence data to this transcriptome was more than 90% for all libraries.

The gene expression data demonstrate consistent results for each treatment with a gradient clustering of replicate samples according to treatment with few outliers (Fig. 2). There is some biological variation between replicates as expected from natural variation in wood and the variation in modification of the wood blocks. The *P. radiata* and WPG37 experiments display a wider range of biological variation compared WPG24 and WPG4.

Differential gene expression and Functional enrichment across treatments. To obtain an overall impression of the entire dataset we ran a multifactorial DE analysis, factoring in time and treatment. Thus, all harvest time points were included for all treatments and we extracted contrasts describing the different modified treatments versus the unmodified *P. radiata* experiment, i.e. WPG4 vs *P. radiata*, WPG24 vs *P. radiata* and WPG37 vs *P. radiata*. (Table 1). Functional

enrichment analyses of the resulting gene lists were inferred using the annotated PFAM domains and GO terms from the annotated transcriptome. Compared to *P. radiata*, the WPG4 showed upregulation of zinc-binding dehydrogenase domains (PF00107.21) and two GO terms related to zinc ion binding and oxidoreductase activity. The same enrichment was also found upregulated in WPG24 and WPG37 when compared to *P. radiata*. In addition, these two latter treatments showed upregulation of more oxidoreductase domains, most in WPG37. No PFAM domains or GO terms were found downregulated in WPG4 or WPG24. However, WPG37 showed a strong downregulation of eight PFAM domains and seven GO terms with functions related to protein and peptide degradation, the ubiquitin-proteasome pathway and the Ras gene family compared to *P. radiata* (Table 1), e.g. two domains related to proteasome (PF10584.4 and PF00227.21) and Ras (PF08477.8 and PF00071.17). These terms were not found among the other comparisons.

As an alternative analysis method to the multifactorial DE analyses above, we also clustered the genes with similar expression profiles. The read counts were grouped into ten clusters (K) for each treatment, and samples from *P. radiata*, WPG4, WPG24 and WPG37 were analyzed separately (Fig. 3). For these clusters we did functional enrichment with PFAM and GO terms (Table S3), and also investigated the placement of known genes related to plant cell wall decay in these clusters (Table S4).

For most of the clusters, an observed pattern of higher expression in one or a few of the harvest points was found (Fig. 3). For *P. radiata*, two clusters were directly linked to wood decay and carbohydrate active enzymes (Table S3). One of these clusters (*P. radiata*-K2) was related to early depolymerization of hemicellulose and pectin (enriched for GH28 and GH43 domains and containing the genes OxaD, Man5a and CE16b; see Table 2 for information about abbreviated gene names) and highly expressed in week 1, while the other cluster (*P. radiata*-K5) was related to later

stages of cellulose depolymerization (enriched for GH3 and hydrolase activity, and containing the genes Cel5b, Cel2, bGlu, Xyl10a, bXyl; Table 2) and was highly expressed in week 2. Similar enrichments were found for two clusters of WPG4 (WPG4-K2 which is highly expressed early, containing Man5a, CE16a and Gal28a and WPG4-K5 which was expressed late in contrast to *P. radiata* and containing OxaD and Xyl10a), however no clusters can be directly compared across treatments. Two clusters in WPG24 also have enrichment for GO terms related to hydrolase activity; WPG24-K3, which is highly induced in week 3 and contains Gal28a and CE16b and WPG24-K9, which is a large group with no specific induction pattern across harvesting points, where all the other specific genes we investigated were placed. The same pattern was demonstrated for WPG37, where all specific genes, except CE16b, were placed in a large group (WPG37-K10) with no specific induction time. WPG37-10 also had enrichment for GO terms such as protein binding, oxidation-reduction processes and catalytic activity (see Table S3 for more details). Functional enrichment was only found for one other cluster of WPG37 (WPG37-K1). This cluster was enriched for functions related to salt and water stress and was highly expressed in the second harvest point, week 6. One cluster with one or a few of the same domains as in cluster WPG37-K1 could be found for all the other treatments (*P. radiata*-K1, WPG4-K6 and WPG24-K3). For the WPG24 this was induced in the first harvest point, thus earlier than for WPG37. In *P. radiata*-K1 and WPG4-K6 there were no clear pattern of induction time for clusters with these stress domains (Fig. 3; Table S3).

Differential gene expression and functional enrichment within treatments. Pair-wise comparisons of different harvest points within treatments revealed large gene expression differences between the first and the later harvest points, for all treatments. In the *P. radiata*

227 experiment, 2450 *R. placenta* genes were differential expressed between week 1 and week 2, while
228 only 10 genes were differential expressed between week 2 and week 3 (Table S5).

229 The furfurylated wood modification demonstrated a similar temporal pattern of DE genes
230 as the *P. radiata* experiment (Table S6). For WPG4 there were 103 DE genes between week 3 and
231 week 6 and 481 DE genes between week 3 and week 9. No DE genes were observed between week
232 6 and week 9. For WPG24, large numbers of DE genes were observed between week 3 and the
233 later time points, but again very few in between the later harvest points. For WPG37, few genes
234 were differentially expressed (between harvest points) in general. However also here, more DE
235 genes were found between week 3 and the later harvest points, and fewer among the later harvest
236 points.

237 Functional enrichment analyses of the pair-wise analyses conformed with the expected two-
238 step decay in this system (Table S7). These results demonstrated that for *P. radiata* experiment
239 there was an increased expression of functions related to hydrolase and catalytic activity from week
240 1 to the later harvest points, especially pronounced in week 2 and week 3 (Table S7). This was also
241 found, but to a lesser extent in WPG4 and WPG24. In WPG4, most of this response was found
242 between week 3 and week 9, while for WPG24, the response mainly started in the comparison
243 between week 3 and week 12 to week 18. For WPG37, this was not pronounced, and no hydrolase
244 activity was enriched. In the first harvest points of the *P. radiata*, WPG4 and WPG24 treatments
245 we found less enrichment of upregulated functions with the exception of some upregulation of GO
246 terms related to protein binding and metal ion binding. However, in WPG37 there was an
247 enrichment of several terms related to iron binding, heme binding, oxidoreductase activity and
248 cytochrome P450s in the upregulated gene set of week 3 compared to week 18. Significant

249 enrichment of a GO term of oxidation-reduction process was found in later stages in WPG4 and
250 WPG24.

251 As week 1 in *P. radiata* was considered the first initial step of decay, with only 0.8% mass
252 loss, we compared *P. radiata* week 1 to all other time points and treatments (Table S8). As with
253 the timeseries analyses, a signal of downregulation of protein degradation was found in all the
254 WPG37 harvest points compared to *P. radiata*. This was seen as enrichment of protein kinases,
255 proteasome, F-box domain and endopeptidase activity in *P. radiata*. This pattern was also found
256 in the early harvest points of WPG24. In contrast week 1 of the *P. radiata* showed upregulation of
257 wood decay related functions as sugar transporters, GHs, and dehydrogenases.

258 **Differential expression of specific genes of interest.** The gene expression of annotated
259 CAZymes that are involved in wood decay according to Floudas et al. (34) were plotted as
260 heatmaps across treatments (Fig. 4). On *P. radiata* the core glycoside hydrolase (GH) enzymes
261 were expressed during intermediate harvest points (week 2 and week 3), while more of the
262 oxidative enzymes where higher expressed early (week 1). When comparing the core enzymes
263 between *P. radiata* and WPG37, in both treatments cellolytic activity was turned off in the late
264 decay stages (*P. radiata* in week 4 and WPG37 in week 15). The oxidative enzymatic apparatus
265 appears to be turned on for longer and does not have a clear induction time in WPG37 compared
266 to *P. radiata*.

267 **Detailed qRT-PCR analyses of key genes of interest.** Large RNAseq datasets tend to
268 contain a lot of biological variation as seen in our PCA plot, which will affect downstream
269 differential expression analyses. qRT-PCR serves both as a RNAseq control but also provides
270 deeper/more detailed insight into the expression of individual genes. Here we have used qRT-PCR

271 primers for key genes involved in wood decay and applied a traditional qRT-PCR approach (Thus
272 the same genes as those reported in the cluster analyses; Table 2; Table S4; Table S9). Plots of both
273 RNAseq and qRT-PCR data for selected genes are provided (Fig. S3-S7). The results below are
274 based on these qRT-PCR data, RNAseq data are commented on when the trends deviated from the
275 qRT-PCR data. It is important to keep in mind that RNAseq and qRT-PCR data are from different
276 wood plugs (n = 4 for both datasets), i.e. the same samples are not used for both analyses. Wood
277 samples for each experiment were selected to keep the variation small within experiments. This
278 caused some variation between the experiments. The main effect believed to be reflected in the
279 results is a slightly faster decay for qRT-PCR WPG37 samples than for the RNAseq WPG37
280 samples. It is also worth to keep in mind that qRT-PCR included an additional harvest point (week
281 21).

282 **Genes involved in oxidative depolymerization: Oxalate synthesis and oxalate**
283 **decomposition.** Oxalic acid is assumed to play an important role as an iron chelator and a phase
284 transfer agent in the CMF system (16, 35). The selected genes involved in *R. placenta* oxalic acid
285 metabolism included glyoxylate dehydrogenase and oxaloacetate dehydrogenase related to oxalic
286 acid synthesis (GlyD, and OahA; Table 2) and oxalate decarboxylase related to oxalic acid
287 degradation (OxaD; Table 2; Fig. S3). GlyD was upregulated in *P. radiata* compared to
288 furfurylated samples (due to the high expression in *P. radiata* at the first harvest point). For *P.*
289 *radiata* and WPG4 GlyD and OahA were upregulated the first harvest points. For WPG24 and
290 WPG37 it seemed to be a delay in expression of OahA, showing an upregulation at the last
291 harvesting points.

292 The expression levels of OxaD in qRT-PCR were low in the present study (or not
293 detectable) and no statistically significant trends were found. The RNAseq data showed a strong

294 induction at early-intermediate stages in the different experiments. The comparison with the lowly
295 expressed qRT-PCR data should be interpreted with caution, but the general trends were similar
296 (Fig. S3).

297 **Genes involved in oxidative depolymerization: Redox enzymes.** Extracellular peroxide
298 generation is a key component of oxidative lignocellulose degradation. The selected genes
299 illustrated in Fig. S4 assumed to be involved in the early oxidative stage of *R. placenta* decay
300 included three GMC oxidoreductases (CAZy family AA3) (AOx1, AOx2, AOx3 and AOx4; Table
301 2), two copper radical oxidases (Cro1, Cro2; Table 2) and a benzoquinone reductase (BqR; Table
302 2).

303 GMC oxidoreductases are flavoenzymes that oxidize a wide variety of alcohols and
304 carbohydrates, with concomitant production of hydrogen peroxide or hydroquinones (36). AOx1
305 and AOx2 were in the present study upregulated in WPG37 compared to *P. radiata*, and for AOx2
306 WPG24 was also upregulated. AOx3 was highly expressed but no significant differences in
307 expression were found within (except an upregulation WPG24 week 3) or between treatments.
308 AOx4 showed low expression levels.

309 Copper radical oxidases (CAZy family AA5) are widely distributed among wood decay
310 fungi (37), and oxidize a variety of substrates and produce H_2O_2. Cro1 and Cro2 were in the present
311 study upregulated week 1 for *P. radiata* and week 21 for WPG24. Since RNAseq was not
312 performed beyond week 18 this trend was not confirmed. Cro2 was upregulated in WPG24
313 compared to WPG4.

314 Benzoquinone reductases (CAZy family AA6) are intracellular enzymes suggested to have
315 a role in degrading lignin and derived compounds in white rot fungi but also suggested to provide

316 protection from oxidative stress by acting as redox active toxins and also contribute to oxidative
317 depolymerization of wood cell wall polymers via the production of hydroquinone chelators (38).
318 In the present study BqR was upregulated in later stages of decay both for *P. radiata* and for
319 WPG37.

320 **Hydrolytic enzymes involved in polysaccharide depolymerization: Hemicellulose and**
321 **pectin degradation.** Fig. S5 illustrates the selected genes involved in hemicellulose hydrolysis.
322 One endomannanase in CAZy family GH5 (Man5a; Table 2) was found to be upregulated in *P.*
323 *radiata* versus WPG37. All treatments showed downregulation with increasing incubation time.

324 For the two endoxylanases in CAZy family GH10 (Xyl10a and Xyl10b; Table 2) there was
325 a tendency for upregulation in furfurylated wood at 3 weeks incubation. For RNAseq an
326 upregulation in *P. radiata* week 2.

327 Betaxylosidase in CAZy family GH3 (bXyl, Table 2) hydrolyses 1,4 beta D-xylans and
328 xylobiose. bXyl was upregulated in WPG37 compared to WPG4. In *P. radiata* there was an
329 upregulation week 3 compared to week 5, while for furfurylated wood there was an upregulation
330 in WPG24 and WPG37 at the last harvest point (week 21).

331 Carbohydrate esterases catalyze the de-O or de-N-acylation of substituted saccharides. The
332 selected carbohydrate esterase CE16a (Table 2) was upregulated in *P. radiata* compared to WPG4
333 and WPG37. All treatments showed downregulation with increasing incubation time. The
334 carbohydrate esterase CE16b (Table 2) provided very low expression levels with qRT-PCR
335 (especially *P. radiata* and WPG4). A clearer trend was found with RNAseq, especially for WPG24
336 and WPG37 with decreasing expression levels with increasing incubation time.

337 Polygalacturonase (Gal28a; Table 2) hydrolyses the alpha-1,4 glycosidic bonds between
338 galacturonic acid residues (pectin). Gal28a was upregulated in *P. radiata* compared to WPG4 and
339 WPG37. All treatments showed downregulation with increasing incubation time.

340 **Hydrolytic enzymes involved in polysaccharide depolymerization: Cellulose**
341 **degradation.** The endoglucanases Cel5a and Cel5b (Table 2) cause chain breaks in amorphous
342 cellulose. Cel5a was upregulated in WPG4 vs. WPG37, and Cel5b was upregulated in *P. radiata*
343 and WPG4 vs. WPG24 and WPG37 (Fig. S6). The expression in *P. radiata* increased with
344 increasing incubation time.

345 Glucoside hydrolase XyGEg (Table 2) shows high sequence similarity to several
346 endoglucanases with activity on cellulose and xyloglucan. This enzyme was upregulated in WPG4
347 vs. WPG37. In *P. radiata* samples it was a gradual increase in XyGEg with increasing incubation
348 time.

349 GH3 Betaglucosidase (bGlu; Table 2) release glucose by hydrolysis of cellobiose and was
350 upregulated in *P. radiata* and WPG4 vs. WPG37. In WPG24 and WPG37 there was an upregulation
351 at week 9 vs. week 21.

352 Lytic polysaccharide monooxygenases (CAZy AA families 9, 10, 11, 13, 14 and 15) are important
353 enzymes in lignocellulose depolymerization, that cause oxidative chain breaks in crystalline and
354 amorphous polysaccharides. We selected a cellulose active AA9 (LPMO; Table 2). For qRT-PCR
355 no statistically significant trends were detected for this gene except for an upregulation week 3 in
356 WPG37.

357 **Expansins with a possible role in loosening plant cell-wall interactions.** Expansins are
358 hypothesized to increase enzyme accessibility by loosening plant cell-wall interactions, although
359 no catalytic mechanism is known (39-41). The two selected genes predicted to encode expansins
360 (Exp1 and Exp2; Table 2) are given in Fig. S7. The expression patterns of the two expansins did
361 not show a clear trend, but for Exp1 in WPG37 the expression was upregulated week 3 and 9
362 compared to later decay stages.

363

DISCUSSION

We have investigated if wood modification by furfuryl alcohol causes altered decomposition response in *Rhodonia (Postia) placenta*, using RNAseq and qRT-PCR, in unmodified and furfurylated *P. radiata* wood.

From our four treatments (*P. radiata*, and the three levels of modification with furfuryl alcohol polymer) we found that WPG4 closely followed the trend on *P. radiata,* while WPG24 seemed to be an accelerated version of the decay pattern of WPG37. For simplicity, we mainly focus on *P. radiata* decay processes and the comparison of *P. radiata* decay vs. WPG37 decay in the discussion.

In our *P. radiata* decay experiments we observed wood decay from incipient stages with mean mass loss of 0.8% in week 1 to severely decayed wood with a mean mass loss of 29% at week 5. Our results support the previously suggested two-step decay mechanism of brown rot fungi (13, 16, 17, 19). Week 1 of *P. radiata* demonstrated an early decay transcriptome response, with higher expression of oxidative enzymes, polygalacturanase GH28 and oxalate synthesis genes in both the RNAseq data and for the specific genes subject to qRT-PCR (Fig. 4; Fig. S4).

This early response was followed by a polysaccharide depolymerization stage, with upregulation of hemicellulases, e.g. endoxylanases (Xyl10b and Xyl10a), beta xylosidase (bXyl) and endomannanase (Man5a) in week 2 and week 3. In our study there was an abrupt downregulation of many core hemicellulases in week 4 during the later stages of decay (Fig. 4, Fig. S6); Xyl10a, Xyl10b, bXyl and Man5a). This is in agreement with observations made by Zhang and Schilling (19). It has been demonstrated that soluble sugars, in particular cellobiose, acts as the main inducing agent in the switch from oxidative (week 1) to hydrolytic depolymerization (19, 42).

386 Cellulose active enzymes were also induced in week 2, and were further upregulated in
387 week 3. This was particularly obvious from the qRT-PCR expression pattern of the GH3
388 betaglucosidase (bGlu), and the LPMO (Fig. S6). Some cellulases are also highly expressed in the
389 more advanced stages of decay, e.g. both the endoglucanase GH5 (Cel5b) and the glucoside
390 hydrolase GH12 (Cel12a) are highest expressed in week 5. This high expression of cellulases at
391 late decay stage was also observed by Zhang and Schilling (19). Thus, when the more easily
392 accessible hemicelluloses have been degraded, expression of cellulases Cel5b and Cel12a are
393 maintained at a high level, well into the phase where the fungus is experiencing starvation
394 (discussed further down).

395 When the decay of the untreated *P. radiata* was compared to the modified wood, we
396 observed that the oxidative enzymes were highly expressed in the first harvest point (week 3) also
397 for the modified WPG37. This is confirming the finding in Alfredsen et al. (28) where *R. placenta*
398 expressed high levels of oxidative enzymes and produced oxalate during 8 weeks colonization of
399 furfurylated Scots pine. However, the pattern of repression of these oxidative processes and the
400 oxalate synthesis found in *P. radiata* at later stages is less clear (Fig. 4). This is particularly obvious
401 when comparing the expression of oxalate decarboxylase (OxaD) and AA3 GMC oxidoreductase
402 (AOx1), which showed a distinct time of induction on *P. radiata* but not on WPG37 where elevated
403 expression was randomly distributed over time between samples. This can conceivably be
404 explained by a repeated exposure to regions with heavily modified substrate, thus re-inducing
405 oxidative processes to overcome furfurylation in order to expose degradable substrate to the fungus
406 allowing further growth, or a direct response to the furfuryl polymer.

407 However, the strong induction of core hydrolyzing enzymes and accessory enzymes
408 observed in week 2 and 3 in *P. radiata* seemed comparable to WPG37 from week 6-12, and

409 partially week 15 as observed by the RNAseq CAZymes analyses and the qRT-PCR analyses (Fig.
410 4, Fig. S6). Thus, the switch to turn on the core hydrolyzing enzymes in the intermediate decay
411 stages was observed in both untreated and furfurylated wood in our experiments, thus we
412 hypothesize that furfurlyation does not influence the availability of these soluble sugars to such an
413 extent that it inhibits induction. Previous studies have showed that *R. placenta* grown on wood
414 modified with both furfurylation and acetylation show similar or decreased levels of core wood
415 hydrolyzing enzymes (26, 28). Our study, with a longer time series, does not suggest reduced
416 expression of these genes, but rather a delayed and elongated process. The elongated process could
417 also be the reason for the placement of all the specific plant cell wall related genes in the large
418 cluster with no obvious induction time in WPG37. The longer incubation times used in this study,
419 and the elongated processes can explain why this trend was never observed in previous studies.
420 Thus, based on the observation that a delayed but, similar pattern was observed in both the *P.*
421 *radiata* and WPG37 experiments, we conclude that the furfurylation does not directly influence
422 the expression of these core PCW degrading enzymes.

423 There are several hypotheses regarding the mode of action of modified wood against brown
424 rot decay fungi (43, 44), summarized in (45). Briefly they hypothesize that: unavailability of easily
425 accessible nutrients (43, 44), enzyme non-recognition (7), micropore blocking (46), and moisture
426 exclusion due to OH-group blocking/reduction (44), and/or reduction in void volume may be
427 important modes of action (47, 48). In our study we have proven that the enzymes do recognize the
428 substrate in the modified treatments, thus we can rule out enzyme non-recognition. The main
429 conclusion from Ringman et al. (45) was that "only one theory provides a consistent explanation
430 for the initial inhibition of brown rot degradation in modified wood, that is, moisture exclusion via
431 the reduction of cell wall voids. Other proposed mechanisms, such as enzyme non-recognition,

micropore blocking, and reducing the number of free hydroxyl groups, may reduce the degradation rate when cell wall water uptake is no longer impeded". The delay in gene expression in our study can be explained by initial blocking of wood polysaccharides by furfuryl alcohol polymers compared to unmodified wood. In addition, a further delay in decay of modified wood versus *P. radiata* is expected due to lower wood moisture content in the modified substrate. Moreover, the strong enrichment of salt stress genetic functions in the WPG37-K1 clustering that was not found in the other treatments may support the conclusions by Ringman et al. (45) that moisture exclusion may be an important mode of action in this modification method.

As a support for the notion that the furfurylation is non-toxic for the fungus, we found no evidence for expression of more defense mechanisms in the modified wood. *Rhodonia placenta* is known to be highly tolerant to substances as copper, mainly due to the ability to produce oxalic acid that chelate and precipitate copper and other transition metals (49). However, in addition to these more general functions that are difficult to separate from wood decay mechanisms, copper tolerant fungi are also known to express catalases and ATP-pumps related to copper transport in response to toxins (50). These functional categories were not enriched in the differential expressed gene sets in our study when comparing WPG37 to the *P. radiata*, indicating that the fungus is not experiencing a more toxic atmosphere in the modified wood.

Notably, the most pronounced transcriptome differences in the *P. radiata* compared to the modified wood is the strong induction of functions related to the ubiquitin/proteasome pathway, protein degradation and the RAS pathway. All these functions are related to carbon starvation and are highly enriched in the late decay of the unmodified *P. radiata*. Thus, we hypothesize that *R. placenta* growing on *P. radiata* is starving and that the fungus has consumed the majority of

454 available carbon sources in the wood in the latest harvest points of the *P. radiata* experiment. This
455 is further supported by the downregulation of CAZymes the last two weeks in this experiment.

456 The ubiquitin/proteasome pathway is a conserved pathway in all eukaryotic organisms, and
457 is important to various cellular processes as recycling of intracellular protein (where unnecessary
458 proteins are degraded to amino acids that can be reused to produce new proteins) and programmed
459 cell death. Recently, the pathway was shown to be activated by carbon starvation in the
460 ectomycorrhizal basidiomycete species *Paxillus involutus* (51). In *P. involutus*, 45% of the
461 transcripts were differentially regulated during carbon starvation. This large response is also shown
462 in our study where most enriched functions in *P. radiata* compared to the WPG37 for the time
463 series analyses could be connected to the U/P or the Ras pathway. This could reflect the higher
464 need for translocation of nitrogen rich resources in the *P. radiata* substrate to areas that need new
465 protein synthesis than is the case in WPG37 or simply reflect a general starving response due to
466 lack of substrate.

467 The other pattern observed as upregulated in *P. radiata* compared to WPG37 was several
468 domains related to Ras proteins. These proteins are involved in cell proliferation and growth of the
469 mycelia. Carbon starvation supports an upregulation of these proteins. In starving mycelia it has
470 been shown that the diameter of the hypha is reduced, while it grows to cover larger area (51, 52).
471 Ras proteins have been shown to enhance the formation of pseudohyphal growth in starving yeast
472 cultures. These pseudohyphae are thin and long cells extending away from the culture, searching
473 for nutrients (53). Ras proteins might well be involved in a change in growth to search for more
474 nutrients in starving mycelia across the fungal kingdom.

475 In all our experiments we have investigated one strain, the FPRL 280. Thaler *et al.* (54)
476 suggested significant differences in the regulation of key lignocellulose degrading enzymes
477 between the previously sequenced MAD-698-R strain and the FPRL 280 strain used in this work.
478 This proposed difference is supported by the current study with a mapping success of only 40-60%
479 when the reads of European strain FPRL 280 were mapped to the genome of MAD 698-R. The
480 difference might have been present since time of isolation or (less likely) the changes might have
481 occurred during storage of these strains. This highlights the importance of providing verifiable
482 strain information when publishing decay studies and when comparing American versus European
483 wood decay testing.

484 Furthermore, for decay testing, the sample size, sample geometry and wood anatomy
485 influence the colonization rate. Sampling time and extent of decay is crucial when examining gene
486 expression or secretome of fungal colonization of wood. The studies by Zhang et al. (17) and Zhang
487 & Shilling (19) used thin wafers and harvested at different distances from the *R. placenta* hyphal
488 front. This wafer approach works relatively well to separate different initial decay stages. For more
489 advanced stages of decay a different approach is needed. In the current study we selected small and
490 homogeneous (earlywood) samples in order to enable fast colonization and as homogenous solid
491 wood substrate for decay as possible. Still, some variation of gene expression is expected as new
492 colonization pathways will be found close to areas with previously colonized wood. This effect is
493 expected to increase with increasing WPG level, since areas long colonized will cease to provide
494 nutrients able sustain survival while the others more recently invaded will provide nutritious
495 substrates. In our experiments, the wood modification treatment modifies the composition of the
496 wood, and the fungus is therefore forced to respond differently than when it encounters unmodified

497 wood. Hence, comparison at similar mass losses between treatments was not the goal of this study,
498 but rather the shift of gene expression over time between and within the different treatments.

499 Increased knowledge about brown rot decay mechanisms is important for an expanded
500 understanding of the fungal decay process in general since ecosystem carbon flows are closely
501 linked to wood degrading fungi. From an industry perspective the findings in this study show that
502 successful inhibition of the initial oxidative decay is a clue to success for future wood protection
503 systems.

504 **CONCLUSIONS**

505 This is the first time the entire gene expression pattern of a decay fungus is followed in untreated
506 and modified wood from initial to advanced stages of decay. From these observations, we have
507 demonstrated how the furfurlyated modification delays the fungus gene expression while growing
508 on this substrate. All treatments (modified and unmodified) expressed the expected staggered decay
509 mechanism, i.e. oxidative enzymes earlier, and then the hydrolyzing enzymes later. Thus, we show
510 that the fungus experiences a similar substrate situation on the modified wood, or at least is
511 following the same modality of gene expression. The major difference is that the responses are
512 delayed and elongated compared to unmodified wood. However, from the downregulation of
513 CAZymes in the latest harvest points in the WPG37, the fungus seems to be finalizing the decay
514 also in the furfurylated wood at a mass loss of only 14%, compared to 29% in *P. radiata*. This
515 suggests that the fungus never get access to the remaining carbohydrates from the modified wood
516 even at low mass loss. The lower levels of modification in the WPG4 and WPG24 treatments show
517 intermediate expression differences and higher mass loss. The mode of action of the modification
518 is still uncertain. However, the similar decay mechanisms, and the lack of expression of defense

519 mechanisms may indicate that the furfurylation functions as both a physical barrier and a factor
520 that creates a less hydrated environment for the fungus. These hypotheses should be investigated
521 to further improve environmentally friendly modification processes.

522

MATERIAL AND METHODS

Wood material. In order to get as homogeneous wood material as possible plugs (Ø = 6 mm, h = 10 mm) were prepared from *Pinus radiata* D. Don earlywood according to Beck et al. 2017 (55). The boards were provided by Kebony ASA, Skien, Norway. Before treatment all samples were dried at 103 °C for 18 hours then cooled down in a desiccator before initial dry weight was recorded. The furfurylation process was performed with three different concentrations of furfuryl alcohol synthesis grade > 98% (Merck, Darmstadt, Germany) according to the formula by Kebony with; furfurylalcohol to water ratio of 7:10 (WPG37) the commercial treatment level, 4:10 (WPG24) and 1:10 (WPG4). The samples were left soaked in the furfuryl alcohol solutions for 15 days. Sets of five samples were wrapped in aluminum foil and cured at 120 °C for 16.5 hours. All samples including *P. radiata* were leached according to EN 84 (1997) as a pre-weathering test and dried at room temperature. In order to provide Weight Present Gain (WPG) and initial dry mass after treatment the samples were dried at 103 °C for 18 hours then cooled down in a desiccator before the dry weight was recorded. The samples were left in a climate chamber at 65% relative humidity and 20 °C until stable weight before they were wrapped in sealed plastic bags and sterilized by gamma irradiation (25 kGY) at the Norwegian Institute for Energy Technology.

Decay test. The brown rot fungus in this experiment was *Rhodonia placenta* (Fr.) Niemelä, K.H. Larss. & Schigel (syn. *Postia placenta*) strain FPRL 280. The fungus was first grown on 4% (w/v) Difco™ malt agar (VWR) media and plugs from actively growing mycelia were transferred to a liquid culture containing 4% (w/v) Difco™ malt (VWR). After two weeks the liquid culture was homogenized with a tissue homogenizer (Ultra-turrax T25, IKA Werke GmbH & Co. KG, Staufen, Germany).

546 A modified E10-16 soil-block test (21) was used. Agar plates (TC Dish 100, standard,
547 Sarstedt AG & Co., Nümbrecht, Germany) (Ø = 87 mm, h = 20 mm) containing soil (2/3 ecological
548 compost soil and 1/3 sandy soil) was adjusted to 95% of its water holding capacity according to
549 ENV 807 (CEN 2001). A plastic mesh was used to avoid direct contact between the samples and
550 the soil. A 300 µl inoculum of homogenized liquid culture was added to each sample. Eight samples
551 of the same treatment were added to each plate and four replicate plates were used.

552 Samples were incubated at 22°C and 70% RH and harvested every third week. Fungal
553 mycelium was manually removed from the wood surface with Delicate Task Wipes (Kintech
554 Science, UK). Eight samples from each treatment and each harvesting point were dried at 103°C
555 for 18 hours in order to provide data for mass loss (mean WPG: WPG4 3.8±0.7, WPG24 24.6±4.1,
556 WPG37 36.1±5.5). The remaining samples were wrapped individually in aluminum foil and put
557 directly into a container with liquid nitrogen. The samples were then stored at -80°C.

558 For RNAseq analyses samples from the following harvesting points were used: *P. radiata*
559 week 1, 2, 3, 4 and 5, WPG4 week 3, 6 and 9, WPG24 week 3, 6, 9, 12, 15 and 18. For qRT-PCR
560 samples from the following harvesting points were used: *P. radiata* week 1, 3 and 5, WPG4 week
561 3, 6 and 9, WPG24 week 3, 9, 15 and 21, WPG37 week 3, 9, 15 and 21.

562 **RNA purification and cDNA synthesis.** Wood powder from frozen samples was obtained
563 by cutting the plugs into smaller pieces with a garden shears wiped with 70% alcohol and thereafter
564 Molecular BioProducts™ RNase AWAY™ Surface Decontaminant (Thermo Scientific,
565 Singapore). The wood samples were immediately cooled down again in Eppendorf Tubes™ in
566 liquid nitrogen. Fine wood powder was produced in a Retsch 300 mill (Retsch mbH, Haan,
567 Germany). The wood samples, the 100-mg stainless steel beads (QIAGEN, Hilden, Germany) and

568 the containers were chilled with liquid nitrogen before grinding at maximum speed for 1.5 min.
569 They were then cooled in liquid nitrogen again before a second round of grinding.

570 For Illumina seq MasterPure^{TM} Plant RNA Purification KIT (epicentre, Madison, WI, USA)
571 was used according to the manufacturer's instruction for total RNA extraction with 100 mg wood
572 sample. Mean WPG for the four replicate samples: WPG4 3.6±0.5, WPG24 24.8±1.2, WPG37
573 39.7±2.2.

574 For qRT-PCR MasterPureTM Complete DNA and RNA Purification KIT (epicenter,
575 Madison, WI, USA) was used according to the manufacturer's instruction with 90 mg wood
576 sample. (A different kit was used because the kit used for Illumina analyses was no longer
577 produced). Mean WPG for the four samples: WPG4 4.1±0,4, WPG24 20.9±0.9, WPG37 33.7±3.8.
578 NanoDrop^{TM} 2000 spectrophotometer (Thermo Scientific, Singapore) was used to quantify RNA
579 in each sample. To convert RNA to cDNA TaqMan Reverse Transcription Reagent KIT (Thermo
580 Scientific, Singapore) was used according to the manufacturer's instructions. Total reaction volume
581 was 50 µl. 300 ng RNA were reacted with oligo $d(T)_{16}$ primer in RNase free water (Qiagene,
582 Hilden, Germany). The solution was incubated two cycles in the PCR machine (GeneAmp® PCR
583 System 9700, Applied Biosystems, Foster City, CA, USA) at 65 °C/5 min and 4 °C/2 min. The
584 PCR machine was paused and the master mix added. The next three cycles included 37 °C/30 min,
585 95 °C/5 min and 4 °C/indefinite time. In addition to the test samples, two samples without RNA
586 were added as controls and used for each primer pair. After the cDNA synthesis, 50 µl RNase free
587 water (Qiagene, Hilden, Germany) was added to the samples and mixed well.

588 **RNAseq sequencing, quality control and trimming.** All Illumina libraries and
589 sequencing were performed by the Norwegian Sequencing Centre (http://www.

sequencing.uio.no). All samples were prepared with the strand specific TruSeq™ RNA-seq library preparation method. In order to produce a high quality *de novo* transcriptome we sequenced the strain grown on a 4% (w/v) Difco™ malt agar (VWR) media in addition to ten selected samples spanning the entire experimental setup on one lane on the Hiseq2500 producing 125 bp paired end sequences. These libraries generated ~395 million read pairs, which after quality control and trimming was reduced to ~250 million read pairs.

For the experiment itself, we collected 80 samples of which three failed library preparation resulting in 77 NextSeq samples in total. The sequenced libraries generated ~28 million trimmed reads on average.

The quality was evaluated using FastQC v. 0.11.2 (56) and trimming performed with Trimmomatic v. 0.36 (57) with the following parameters: TruSeq3-SE.fa:2:30:10 MAXINFO:30:0.4 MINLEN:30 for the NextSeq samples. For the Hiseq2500 samples, the built-in trimmomatic option in Trinity v. 2.2.0 (58) with the following parameters: TruSeq3-PE.fa:2:30:10 SLIDINGWINDOW:4:5 LEADING:5 TRAILING:5 MINLEN:30 MAXINFO:30:0.4 was used.

Transcriptome assembly and evaluation. We initially attempted to use the *R. placenta* genome generated from an American *R. placenta* strain in our analysis (Postia_placenta_mad_698, full fasta sequence (soft masked) from the Ensembl fungi FTP server). The genome-based attempt using Bowtie2, Tophat2 and Cufflinks resulted in very poor mapback (~50-70 %) despite doing parameter sweeps (data not shown). We also attempted to use the genome-guided option of the *de novo* transcriptome assembler Trinity that yielded a more fragmented transcriptome compared to the clean *de novo* version (data not shown).

611 The final transcriptome was generated using a *de novo* strategy with the HiSeq trimmed
612 reads and Trinity v. 2.2.0 (seqType fq, max_memory 250G, SS_lib_type RF, CPU 20,
613 bflyHeapSpaceMax 10G and bflyCPU 20) on our local computing cluster. The Trinity bfly process
614 failed for 110 elements which were rerun with more memory. The finished transcriptome contained
615 56 520 contigs (Table S1).

616 We also evaluated the assembly using BUSCO v. 2.0 using the recommended parameters
617 and the corresponding fungi database created 26th of January 2017 with 85 species and 290 BUSCO
618 genes (59). Of the 290 BUSCO genes 288 were found complete (99.3 %) (Table S2).

619 **Assembly annotation using Trinotate and the JGI Fungi Portal.** The assembly was
620 subjected to the Trinotate annotation pipeline according to the manual which provided a generic
621 annotation of assembly. However, as there is a study (17) looking into key wood-degrading genes
622 using the annotation from the *R. placenta* genome, we manually annotated our assembly using the
623 predicted proteins reported at the JGI Fungi Portal
624 (https://genome.jgi.doe.gov/programs/fungi/index.jsf) using TBLASTN from BLAST+ (60) with
625 an e-value cutoff 1e-50. Finally, we ended up with a custom annotation being a hybrid of the
626 generic trinotate annotation where identifiers from the *R. placenta* genome have been added.
627 Finally, we manually evaluated the hits from the key genes reported in Zhang *et al.* (17) to
628 overwrite any generic annotation provided by trinotate as these have been manually verified and
629 submitted to the CAZy database (http://www.cazy.org/).

630 **Mapping and abundance estimation of NextSeq samples.** Mapping was performed using
631 the built-in mapping option in Trinity v. 2.3.2 with the RSEM count estimation method, the bowtie
632 alignment method and specifying SS_lib_type R. The counts were collected per 'gene' using the

633 abundance_estimates_to_matrix.pl script in Trinity and the resulting count matrix used for
634 differential gene expression in R.

635 **Differential gene expression analysis.** In R v3.4.1 the overall data was initially explored
636 using VarianceParition v1.8 (61). Differential gene expression analyses were performed using
637 edgeR v 3.20.1 (62, 63). In addition some of the plot functions in DESeq2 v1.18.0 (64) were used
638 to explore that overall data and to plot raw counts.

639 The overall workflow with code is available in the supplementary information, but briefly
640 we followed the steps described below:

641 The coldata object describing the overall experiment was set up with time, treatment, mass
642 loss and condition where condition in practice is the intercept between time and treatment. We
643 initially filtered on counts per million (CPM, cutoff = 1 in at least 2 libraries) and set a full model
644 consisting of treatment, time, condition and mass loss to explore the data in variancePartition. We
645 also made heatmaps using pheatmap v1.0.8 and log2 transformed count data.

646 Multifactorial differential expression analysis was performed both in EdgeR and DESeq2
647 (the latter to enable use of various plot functions). In DESeq we opted for a ~treatment+time
648 formula. Running a more complex design with interaction (:) was not possible as DESeq2 cannot
649 handle partial models (time points for the different treatments do not overlap completely).
650 Furthermore, we opted for the likelihood ratio test (LRT) which examines two models for the
651 counts - the full model and a reduced model. This then determines if the increased likelihood of
652 the data using the extra term(s) in the full model is more than expected.

In edgeR we opted for a ~0 + treatment+time formula without generating an intercept term. When estimating overall dispersion, we used the robust=TRUE option to better handle outliers in the data. For the multifactorial test itself we chose to replace the standard glmFit with glmQLFit which uses a quasi-likelihood F-test on the likelihood ratio statistics instead of the chisquare approximation. In this way we should obtain a more conservative control of the type I error rate as it takes into account the uncertainty in estimating dispersion for each gene - especially when the number of replicates is small.

To enable exploration of specific contrasts between given conditions we also ran a ~0 + condition formula in edgeR using the same setup as described above.

We evaluated each treatment vs the *P. radiata* over time from the treatment+time multifactorial analysis. For the pairwise contrasts between harvest time within treatments we used the ~condition multifactorial analysis.

The overall exploration of the data revealed that the WPG24 treatment series has a few outliers. RNAseq data is highly variable and the individual variation between replicates can be large. We found that 2 replicates in the WPG24 3 weeks condition were relatively deviating from the other two replicates. We reran the above described analysis without the most extreme outlier (WPG24 3 weeks replicate 2) and observed a large change in the number of reported significant differentially expressed genes. However, as these differences not necessary improved the results we decided to keep all samples in the final dataset.

Clustering using MCDluster.seq. As an alternative to the pair-wise differential expression analyses the read count data were clustered based on similarity in expression patterns using the MBCluster.seq package in R. The EM clustering algorithm was used.

675 **Functional summary.** Functional enrichment analysis was used to characterize function of
676 the differential expressed genes of the various treatments and clusters. A Python script was used to
677 perform functional enrichment analysis of PFAM domains and GO terms using Fisher's exact test
678 (http://cgrlucb.wikispaces.com/Functional+Enrichment+Analysis).

679 **CAZyme annotations.** The transcripts were translated using TransDecoder
680 (https://github.com/TransDecoder/TransDecoder/wiki). All protein sequences were annotated in
681 dbCAN2 (65). The standardized (median/median absolute deviation) gene expression patterns of
682 the resulting annotated transcripts were plotted using in a heatmap using R (66).

683 **qRT-PCR.** The qRT-PCR specific primers used to determine the transcript levels of
684 selected genes were designed with a target T_m of 60°C and to yield a 150 base pair product. qRT-
685 PCR was performed using ViiA 7 by Life technologies (Applied Biosystems, Foster City, CA,
686 USA). The master mix included for each sample: 5 µl Fast SYBR®Green Master Mix (Thermo
687 Scientific, Singapore), 0.006 µl 10 µM forward primer, 0.006 µl 10 µM reverse primer, 2.88 µl
688 RNase free water (Qiagene, Hilden, Germany) and 2 µl test sample (total volume 10 µl). The qRT-
689 PCR run included the following stages: Hold stage with initial ramp rate 2.63 °C/s, then 95.0 °C
690 for 20 seconds. PCR stage with 40 cycles of initial ramp rate 2.63 °C/s, 95.0 °C, ramp rate of 2.42
691 °C followed by 60.0 °C for 20 seconds. The melt curve stage had an initial ramp rate of 2.63 °C/s
692 then 95.0 °C for 15 seconds, ramp rate of 2.42 °C/s 60.0 ° for one second, then 0.05 °C/s.

693 Two constitutive housekeeping genes, β-tubulin - βt (113871) and α-tubulin α-t (123093)
694 were used as a baseline for gene expression. The target genes (Tg) and the endogenous controls in
695 this study are listed in Table 1. Protein ID according to *Postia placenta* MAD 698-R v1.0 genome,
696 The Joint Genome Institute (https://genome.jgi.doe.gov/pages/search-for-

genes.jsf?organism=Pospl1). Threshold cycle values (C_t) obtained here were used to quantify gene expression.

Software used to export the Ct values was QuantStudioTM Real-Time PCR System (Applied Biosystems by Thermo Fiches Scientific, Foster City, CA, USA). Ct-value of βt, αt and Tg were used to quantify gene expression according to the following equation; $10^4 \times 2^{C_t\beta t - C_t Tg}$, giving an arbitrary baseline expression of β-tubulin and α-tubulin of 104. As an internal control, the expression of βt and αt was compared using the same equation, showing a stable expression, with αt being expressed at approximately 80% relative to βt. Only data for βt was included in this paper.

Statistical analysis of qRT-PCR. All statistics were performed in JMP (Version Pro 13, SAS Institute Inc., Cary, NC, USA). Significance of differences in expression levels of each gene were calculated with Tukey honest significant difference (HSD) test. A probability of ≤ 0.05 was the statistical type-I error level.

DATA AVAILABILITY

RNA-seq data generated for this study were deposited at the Sequence Read Archive under accession XXXXXX. The transcriptome assembly and all lists of differentially expressed genes were deposited in Dryad under accession doi:XXXXXX.

ACKNOWLEDGEMENT

717 Thanks to Sigrun Kolstad and Inger Heldal (NIBIO) for help with RNA purification and qRT-PCR.

718 Thanks to Stig Lande (Kebony) for helpful discussions regarding treatment of the samples. This

719 project was financed by The Research Council of Norway 243663/E50 BioMim.

720

721 **REFERENCES**

722 1. **Kutnik M**, **Klamer M**, **Melcher E**. 2017. Ensuring quality of treated wood - regulations,
723 certifications and associative background in the field of wood protection in Europe, p. 15.
724 *In*. Proceedings from the IRG48 Scientific Conference on Wood Protection, Ghent,
725 Belgium, 4-8 June 2017, IRG/WP 17-20626.

726 2. **Sandberg D**, **Kutnar A**, **Mantanis G**. 2017. Wood modification technologies - a review.
727 iForest - Biogeosciences and Forestry **10**:895–908.

728 3. **Hill CAS**. 2006. Wood modification: chemical, thermal and other processes. John Wiley
729 and Sons, Sussex, UK.

730 4. **Lande S**. 2008. Furfurylation of wood – wood modification by the use of furfuryl alcohol.
731 Dr. Scient Thesis. Norwegian University of Life Sciences, Ås, Norway.

732 5. **Nordstierna L**, **Lande S**, **Westin M**. 2008. Towards novel wood-based materials: chemical
733 bonds between lignin-like model molecules and ply (furfuryl alcohol) studied by NMR.
734 Holzforschung **62**:709–713.

735 6. **Lande S**, **Westin M**, **Schneider M**. 2004. Properties of furfurylated wood. Scandinavian
736 Journal of Forest Research **19**:22–30.

737 7. **Rowell RM**. 2012. Handbook of wood chemistry and wood composites, 2nd ed. CRC Press,
738 Taylor and Francis Group, Boca Raton, FL, USA.

739 8. **Riley R**, **Salamov AA**, **Brown DW**, **Nagy LG**, **Floudas D**, **Held BW**, **Levasseur A**,
740 **Lombard V**, **Morin E**, **Otillar R**, **Lindquist EA**, **Sun H**, **LaButti KM**, **Schmutz J**,
741 **Jabbour D**, **Luo H**, **Baker SE**, **Pisabarro AG**, **Walton JD**, **Blanchette RA**, **Henrissat B**,
742 **Martin F**, **Cullen D**, **Hibbett DS**, **Grigoriev IV**. 2014. Extensive sampling of
743 basidiomycete genomes demonstrates inadequacy of the white-rot/brown-rot paradigm for
744 wood decay fungi. Proceedings of the National Academy of Sciences of the United States
745 of America **111**:9923–9928.

746 9. **Gilbertson RL**. 1980. Wood-rotting fungi of North America. Mycologia **72**:1–49.

747 10. **Zabel RA**, **Morrell JJ**. 1992. Wood Microbiology: Decay and its Prevention. Academic
748 Press, San Diego, CA.

749 11. **Wilcox WW**. 1978. Review of literature on the effects of early stages of decay on wood
750 strength. Wood and Fiber Science **9**:252–257.

751 12. **Winandy J**, **Morrell JJ**. 1993. Relationship between incipient decay, strength and chemical
752 composition of douglas-fir heartwood. Wood and Fiber Science **25**:278–288.

753 13. **Goodell B**, **Jellison J**, **Liu J**, **Daniel G**, **Paszczynski A**, **Fekete F**, **Krishnamurthy S**, **Jun**
754 **L**, **Xu G**. 1997. Low molecular weight chelators and phenolic compounds isolated from

wood decay fungi and their role in the fungal biodegradation of wood. Journal of Biotechnology **53**:133–162.

14. **Arantes V**, **Milagres AMF**, **Filley TR**, **Goodell B**. 2011. Lignocellulosic polysaccharides and lignin degradation by wood decay fungi: the relevance of nonenzymatic Fenton-based reactions. Journal of Industrial Microbiology and Biotechnology **38**:541–555.

15. **Eastwood DC**, **Floudas D**, **Binder M**, **Majcherczyk A**, **Schneider P**, **Aerts A**, **Asiegbu FO**, **Baker SE**, **Barry K**, **Bendiksby M**, **Blumentritt M**, **Coutinho PM**, **Cullen D**, **de Vries RP**, **Gathman A**, **Goodell B**, **Henrissat B**, **Ihrmark K**, **Kauserud H**, **Kohler A**, **LaButti K**, **Lapidus A**, **Lavin JL**, **Lee Y-H**, **Lindquist E**, **Lilly W**, **Lucas S**, **Morin E**, **Murat C**, **Oguiza JA**, **Park J**, **Pisabarro AG**, **Riley R**, **Rosling A**, **Salamov A**, **Schmidt O**, **Schmutz J**, **Skrede I**, **Stenlid J**, **Wiebenga A**, **Xie X**, **Kues U**, **Hibbett DS**, **Hoffmeister D**, **Hogberg N**, **Martin F**, **Grigoriev IV**, **Watkinson SC**. 2011. The plant cell wall-decomposing machinery underlies the functional diversity of forest fungi. Science **333**:762–765.

16. **Arantes V**, **Goodell B**. 2014. Current Understanding of Brown-Rot Fungal Biodegradation Mechanisms: A Review, pp. 3–21. *In* Deterioration and Protection of Sustainable Biomaterials. American Chemical Society, Washington, DC.

17. **Zhang J**, **Presley GN**, **Hammel KE**, **Ryu J-S**, **Menke JR**, **Figueroa M**, **Hu D**, **Orr G**, **Schilling JS**. 2016. Localizing gene regulation reveals a staggered wood decay mechanism for the brown rot fungus *Postia placenta*. Proceedings of the National Academy of Sciences of the United States of America **113**:10968–10973.

18. **Goodell B**, **Zhu Y**, **Kim S**, **Kafle K**, **Eastwood D**, **Daniel G**, **Jellison J**, **Yoshida M**, **Groom L**, **Pingali SV**, **O'Neill H**. 2017. Modification of the nanostructure of lignocellulose cell walls via a non-enzymatic lignocellulose deconstruction system in brown rot wood-decay fungi. Biotechnology of Biofuels **10**:179.

19. **Zhang J**, **Schilling JS**. 2017. Role of carbon source in the shift from oxidative to hydrolytic wood decomposition by *Postia placenta*. Fungal Genetics and Biology **106**:1–8.

20. **CEN**. 1996. Wood preservatives - Test method for determining the protective effectiveness against wood destroying basidiomycetes - Determination of toxic values. European Committee for Standardization, Brussels, Belgium.

21. **AWPA**. AWPA E10-16 Laboratory method for evaluating the decay resistance of wood-based materials against pure basidiomycete cultures: Soil/Block test. American Wood Protection Association, Birmingham, AL, USA.

22. **Gaskell J**, **Kersten P**, **Larrondo LF**, **Canessa P**, **Martinez D**, **Hibbett D**, **Schmoll M**, **Kubicek CP**, **Martinez AT**, **Yadav J**, **Master E**, **Magnuson JK**, **Yaver D**, **Berka R**, **Lail K**, **Chen C**, **LaButti K**, **Nolan M**, **Lipzen A**, **Aerts A**, **Riley R**, **Barry K**, **Henrissat B**, **Blanchette R**, **Grigoriev IV**, **Cullen D**. 2017. Draft genome sequence of a monokaryotic model brown-rot fungus *Postia* (*Rhodonia*) *placenta* SB12. Genomics Data **14**:21–23.

23. **Martinez D**, **Challacombe J**, **Morgenstern I**, **Hibbett D**, **Schmoll M**, **Kubicek CP**, **Ferreira P**, **Ruiz-Duenas FJ**, **Martinez AT**, **Kersten P**, **Hammel KE**, **Vanden Wymelenberg A**, **Gaskell J**, **Lindquist E**, **Sabat G**, **Splinter BonDurant S**, **Larrondo LF**, **Canessa P**, **Vicuna R**, **Yadav J**, **Doddapaneni H**, **Subramanian V**, **Pisabarro AG**, **Lavin JL**, **Oguiza JA**, **Master E**, **Henrissat B**, **Coutinho PM**, **Harris P**, **Magnuson JK**, **Baker SE**, **Bruno K**, **Kenealy W**, **Hoegger PJ**, **Kues U**, **Ramaiya P**, **Lucas S**, **Salamov A**, **Shapiro H**, **Tu H**, **Chee CL**, **Misra M**, **Xie G**, **Teter S**, **Yaver D**, **James T**, **Mokrejs M**, **Pospisek M**, **Grigoriev IV**, **Brettin T**, **Rokhsar D**, **Berka R**, **Cullen D**. 2009. Genome, transcriptome, and secretome analysis of wood decay fungus *Postia placenta* supports unique mechanisms of lignocellulose conversion. Proceedings of the National Academy of Sciences of the United States of America **106**:1954–1959.

24. **Vanden Wymelenberg A**, **Gaskell J**, **Mozuch M**, **Sabat G**, **Ralph J**, **Skyba O**, **Mansfield SD**, **Blanchette RA**, **Martinez D**, **Grigoriev I**, **Kersten PJ**, **Cullen D**. 2010. Comparative transcriptome and secretome analysis of wood decay fungi *Postia placenta* and *Phanerochaete chrysosporium*. Applied and Environmental Microbiology **76**:3599–3610.

25. **Vanden Wymelenberg A**, **Gaskell J**, **Mozuch M**, **BonDurant SS**, **Sabat G**, **Ralph J**, **Skyba O**, **Mansfield SD**, **Blanchette RA**, **Grigoriev IV**, **Kersten PJ**, **Cullen D**. 2011. Significant alteration of gene expression in wood decay fungi *Postia placent*a and *Phanerochaete chrysosporium* by plant species. Applied and Environmental Microbiology **77**:4499–4507.

26. **Ringman R**, **Pilgård A**, **Richter K**. 2014. Effect of wood modification on gene expression during incipient *Postia placenta* decay. International Biodeterioration & Biodegradation **86**:86–91.

27. **Ringman R**, **Pilgård A**, **Kölle M**, **Brischke C**, **Richter K**. 2016. Effects of thermal modification on *Postia placenta* wood degradation dynamics: measurements of mass loss, structural integrity and gene expression. Wood Science and Technology **50**:385–397.

28. **Alfredsen G**, **Fossdal CG**, **Nagy NE**, **Jellison J**, **Goodell B**. 2016. Furfurylated wood: impact on *Postia placenta* gene expression and oxalate crystal formation. Holzforschung **70**:947.

29. **Alfredsen G**, **Pilgård A**. 2014. *Postia placenta* of acetic anhydride modified wood – effect of leaching. Wood Material Science and Engineering, **9**: 162-169.

30. **Alfredsen G**, **Pilgård A**, **Fossdal CG**. 2016. Characterisation of *Postia placenta* colonisation during 36 weeks in acetylated southern yellow pine sapwood at three acytelation levels including genomic DNA and gene expression quantification of the fungus. Holzforschung **70**:1055–1065.

31. **Alfredsen G**, **Fossdal CG**. 2009. *Postia placenta* gene expression of oxidative and carbohydrate metabolism related genes during growth in furfurylated wood, p. 7. *In*. Proceedings from the IRG40 Scientific Conference on Wood Protection, Beijing, China, 24-28 May 2009, IRG/WP 09-10701

832 33. **Skyba O**, **Cullen D**, **Douglas CJ**, **Mansfield SD**. 2016. Gene expression patterns of wood
833 decay fungi *Postia placenta* and *Phanerochaete chrysosporium* are influenced by wood
834 substrate composition during degradation. Applied and Environmental Microbiology
835 **82**:4387–4400.

836 34. **Floudas D**, **Held BW**, **Riley R**, **Nagy LG**, **Koehler G**, **Ransdell AS**, **Younus H**, **Chow J**,
837 **Chiniquy J**, **Lipzen A**, **Tritt A**, **Sun H**, **Haridas S**, **LaButti K**, **Ohm RA**, **Kues U**,
838 **Blanchette RA**, **Grigoriev IV**, **Minto RE**, **Hibbett DS**. 2015. Evolution of novel wood
839 decay mechanisms in Agaricales revealed by the genome sequences of *Fistulina hepatica*
840 and *Cylindrobasidium torrendii.* Fungal Genetics and Biology **76**:78–92.

841 35. **Shimanda M**, **Akamtsu Y**, **Tokimatsu T**, **Mii K**, **Hattori T**. 1997. Possible biochemical
842 roles of oxalic acid as a low molecular weight compound involved in brown-rot and white-
843 rot wood decays. Journal of Biotechnology **53**:103–113.

844 36. **Cavener, DR**.1992. GMC oxidoreductases: a newly defined family of homologous
845 proteins with diverse catalytic activities. Journal of Molecular Biology **223**:811-814.

846 37. **Kersten P**, **Cullen D**. 2014. Copper radical oxidases and related extracellular
847 oxidoreductases of wood-decay Agaricomycetes. Fungal Genetics and Biology **72**:124–130.

848 38. **Kameshwar AKS**, **Qin W**. 2016. Lignin Degrading Fungal Enzymes, pp. 81–130. *In* Fang,
849 Z, Smith Richard L, J (eds.), Production of Biofuels and Chemicals from Lignin. Springer
850 Singapore, Singapore.

851 39. **Rose**, **Bennett**. 1999. Cooperative disassembly of the cellulose-xyloglucan network of
852 plant cell walls: parallels between cell expansion and fruit ripening. Trends in Plant
853 Science **4**:176–183.

854 40. **Baker JO**, **King MR**, **Adney WS**, **Decker SR**, **Vinzant TB**, **Lantz SE**, **Nieves RE**,
855 **Thomas SR**, **Li L-C**, **Cosgrove DJ**, **Himmel ME**. 2000. Investigation of the cell-wall
856 loosening protein expansin as a possible additive in the enzymatic saccharification of
857 lignocellulosic biomass. Applied Biochemistry and Biotechnology **84**:217–223.

858 41. **Arantes V**, **Saddler JN**. 2010. Access to cellulose limits the efficiency of enzymatic
859 hydrolysis: the role of amorphogenesis. Biotechnology and Biofuels **3**:4.

860 42. **Benocci T**, **Aguilar-Pontes MV**, **Zhou M**, **Seiboth B**, **de Vries RP**. 2017. Regulators of
861 plant biomass degradation in ascomycetous fungi. Biotechnology and Biofuels **10**:152.

862 43. **Boonstra MJ**, **van Acker J**, **Kegel E**, **Stevens M**. 2007. Optimisation of a two-stage heat
863 treatment process: durability aspects. Wood Science and Technology **41**:31–57.

864 44. **Rowell RM**, **Ibach RE**, **McSweeny J**, **Nilsson T**. 2009. Understanding decay resistance,
865 dimensional stability and strength changes in heat-treated and acetylated wood, pp. 489–
866 502. *In*. The European Conference on Wood Modification, Stockholm, Sweden.

867 45. **Ringman R**, **Pilgård A**, **Brischke C**, **Richter K**. 2014. Mode of action of brown rot decay
868 resistance in modified wood: a review. Holzforschung **68**:239–246.

869 46. **Hill CAS**, **Forster SC**, **Farahani MRM**, **Hale MDC**, **Ormondroyd GA**, **Williams GR**.
870 2005. An investigation of cell wall micropore blocking as a possible mechanism for the
871 decay resistance of anhydride modified wood. International Biodeterioration &
872 Biodegradation **55**:69–76.

873 47. **Boonstra MJ**, **Tjeerdsma B**. 2006. Chemical analysis of heat treated softwoods. Holz als
874 Roh- und Werkstoff **64**:204.

875 48. **Hill CAS**. 2009. Why does acetylation protect wood from microbiological attack? Wood
876 Material Science & Engineering **4**:37–45.

877 49. **Green F III**, **Clausen CA**. 2003. Copper tolerance of brown-rot fungi: time course of oxalic
878 acid production. International Biodeterioration & Biodegradation **51**:145–149.

879 50. **Akgul A**, **Akgul A**, **Tang JD**, **Diehl SV**. 2018. Gene expression analysis of wood decay
880 fungus *Fibroporia radiculosa* grown in ACU-treated wood. Wood and Fiber Science **50**:1–
881 12.

882 51. **Ellström M**, **Shah F**, **Johansson T**, **Ahrén D**, **Persson P**, **Tunlid A**. 2015. The carbon
883 starvation response of the ectomycorrhizal fungus *Paxillus involutus*. FEMS Microbiology
884 Ecology **91**:fiv027.

885 52. **Nitsche BM**, **Jørgensen TR**, **Akeroyd M**, **Meyer V**, **Ram AF**. 2012. The carbon starvation
886 response of *Aspergillus niger* during submerged cultivation: Insights from the transcriptome
887 and secretome. BMC Genomics **13**:380–380.

888 53. **Gimeno CJ**, **Ljungdahl PO**, **Styles CA**, **Fink GR**. 1992. Unipolar cell divisions in the
889 yeast *S. cerevisiae* lead to filamentous growth: Regulation by starvation and RAS. Cell
890 **68**:1077–1090.

891 54. **Thaler N**, **Alfredsen G**, **Fossdal CG**. 2012. Variation in two *Postia placenta* strains, MAD-
892 698-R and FPRL 280 - mass loss, DNA content and gene expression, p. 9. *In*. Proceedings
893 from the IRG43 Scientific Conference on Wood Protection, Kuala Lumpur, Malaysia. May
894 6-10. IRG/WP 12-10781.

895 55. **Beck G**, **Thybring EE**, **Thygesen LG**, **Hill C**. 2017. Characterization of moisture in
896 acetylated and propionylated radiata pine using low-field nuclear magnetic resonance
897 (LFNMR) relaxometry. Holzforschung **72**:225.

898 56. **Andrews S**. 2010. FastQC: a quality control tool for high throughput sequence data.
899 Available online at: http://www.bioinformatics.babraham.ac.uk/projects/fastqc.

900 57. **Bolger AM**, **Lohse M**, **Usadel B**. 2014. Trimmomatic: a flexible trimmer for Illumina
901 sequence data. Bioinformatics **30**:2114–2120.

902 58. **Grabherr MG**, **Haas BJ**, **Yassour M**, **Levin JZ**, **Thompson DA**, **Amit I**, **Adiconis X**,
903 **Fan L**, **Raychowdhury R**, **Zeng Q**, **Chen Z**, **Mauceli E**, **Hacohen N**, **Gnirke A**, **Rhind**
904 **N**, **di Palma F**, **Birren BW**, **Nusbaum C**, **Lindblad-Toh K**, **Friedman N**, **Regev A**. 2011.
905 Full-length transcriptome assembly from RNA-Seq data without a reference genome. Nature
906 Biotechnology **29**:644–652.

907 59. **Simao FA**, **Waterhouse RM**, **Ioannidis P**, **Kriventseva EV**, **Zdobnov EM**. 2015.
908 BUSCO: assessing genome assembly and annotation completeness with single-copy
909 orthologs. Bioinformatics **31**:3210–3212.

910 60. **Camacho C**, **Coulouris G**, **Avagyan V**, **Ma N**, **Papadopoulos J**, **Bealer K**, **Madden TL**.
911 2009. BLAST+: architecture and applications. BMC Bioinformatics **10**:421.

912 61. **Hoffman GE**, **Schadt EE**. 2016. variancePartition: interpreting drivers of variation in
913 complex gene expression studies. BMC Bioinformatics **17**:483.

914 62. **Robinson MD**, **McCarthy DJ**, **Smyth GK**. 2010. edgeR: a Bioconductor package for
915 differential expression analysis of digital gene expression data. Bioinformatics **26**:139–140.

916 63. **McCarthy DJ**, **Chen Y**, **Smyth GK**. 2012. Differential expression analysis of multifactor
917 RNA-Seq experiments with respect to biological variation. Nucleic Acids Research
918 **40**:4288–4297.

919 64. **Love MI**, **Huber W**, **Anders S**. 2014. Moderated estimation of fold change and dispersion
920 for RNA-seq data with DESeq2. Genome Biology **15**:550.

921 65. **Zhang H**, **Yohe T**, **Huang L**, **Entwistle S**, **Wu P**, **Yang Z**, **Busk PK**, **Xu Y**, **Yin Y**. 2018.
922 dbCAN2: a meta server for automated carbohydrate-active enzyme annotation. Nucleic
923 Acids Research **46**:95-101.

924 66. **R Core Team**. R: A language and environment for statistical computing.
925 https://www.R-project.org/
926

927

928

929

930

931

Table 1. Functional enrichment analyses of GO terms and PFAM domains of significant differential expressed genes between treatments along the time series of *Rhodinia placenta* growing on unmodified and three different levels of modification with furfuryl alcohol (Weight Percent Gain (WPG) of wood of 4, 24 and 37%). Description indicates gene ontology variables; MF – Molecular function, BP – Biological process.

Treatment comparison	# DE genes	GO terms and PFAM domains	Frequency	Adjusted p-value	Description	Comment
DOWN WPG4 –UP *P.radiata*	38	No enrichment				
UP WPG4– DOWN *P. radiata*	32	GO:0008270	8/562 (1.42%)	4.699815e-03	MF	Zinc ion binding
		GO:0016491	8/736 (1.09%)	3.389974e-02	MF	Oxidoreductase activity
		PF00107.21	4/76 (5.26%)	1.536767e-02		Zinc-binding dehydrogenase
UP WPG24 – DOWN *P. radiata*	228	GO:0016491	40/736 (5.43%)	9.508001e-13	MF	Oxidoreductase activity
		GO:0055114	46/1163 (3.96%)	5.487584e-10	BP	Oxidation-reduction process
		PF00107.21	12/76 (15.79%)	4.007640e-07		Zinc-binding dehydrogenase
		PF13602.1	7/30 (23.33%)	1.059814e-04		Zinc-binding dehydrogenase
		PF00106.20	13/198 (6.57%)	3.016412e-03		Short chain dehydrogenase
		PF08659.5	11/142 (7.75%)	3.531839e-03		KR domain
		PF13561.1	9/105 (8.57%)	1.170520e-02		Zinc-binding dehydrogenase
DOWN WPG24 – UP *P. radiata*	241	No enrichment				
UP WPG37 – DOWN *P. radiata*	907	GO:0016491	88/736 (11.96%)	6.355618e-19	MF	Oxidoreductase activity
		GO:0055114	108/1163 (9.29%)	2.403803e-15	BP	Oxidation-reduction process
		GO:0016705	38/326 (11.66%)	1.483503e-06	MF	Oxidoreductase activity
		GO:0055085	46/490 (9.39%)	2.946082e-05	BP	Transmembrane transport
		GO:0005506	38/367 (10.35%)	3.882514e-05	MF	Iron ion binding
		GO:0020037	40/419 (9.55%)	1.559430e-04	MF	Heme binding
		GO:0008152	49/664 (7.38%)	1.270725e-02	BP	Metabolic process
		GO:0010181	10/54 (18.52%)	3.305432e-02	MF	FMN binding
		PF08659.5	27/142 (19.01%)	7.135697e-08		KR domain
		PF00106.20	30/198 (15.15%)	2.054525e-06		Short chain dehydrogenase
		PF00107.21	17/76 (22.37%)	1.773561e-05		Zinc-binding dehydrogenase
		PF07690.11	29/222 (13.06%)	1.097127e-04		Major facilitator family
		PF00067.17	35/309 (11.33%)	2.032395e-04		Cytochrome P450
		PF13417.1	9/24 (37.50%)	3.098329e-04		Glutathione S-transferase
		PF13561.1	18/105 (17.14%)	5.010722e-04		Zinc-binding dehydrogenase
		PF00724.15	8/24 (33.33%)	3.857038e-03		NADH: flavin oxidoreductase

		PF13602.1	8/30 (26.67%)	2.424490e-02		Zinc-binding dehydrogenase
DOWN WPG37 – UP *P. radiata*	1125	GO:0006511	18/86 (20.93%)	1.690517e-03	BP	Ubiquitin-dependent protein catabolic process
		GO:0005839	9/23 (39.13%)	2.523168e-03	CC	Proteasome core complex
		GO:0051603	9/23 (39.13%)	2.523168e-03	BP	Proteolysis involved in cellular protein catabolic process
		GO:0019773	6/10 (60.00%)	5.541878e-03	CC	Proteasome core complex, alpha-subunit complex
		GO:0004175	6/11 (54.55%)	1.158001e-02	MF	Endopeptidase activity
		GO:0004298	9/28 (32.14%)	1.630679e-02	MF	Threonine-type endopeptidase activity
		GO:0033178	5/8 (62.50%)	2.652523e-02	CC	Proton-transporting two-sector ATPase complex, catalytic domain
		PF10584.4	6/8 (75.00%)	1.571873e-03		Proteasome A_N
		PF00227.21	9/21 (42.86%)	2.650923e-03		Proteasome
		PF08477.8	16/68 (23.53%)	5.702283e-03		Ras of Complex, Roc, domain of DAPkinase
		PF00009.22	13/49 (26.53%)	9.992408e-03		GTP-binding elongation factor family, EF-Tu/EF-1A subfamily
		PF00025.16	16/74 (21.62%)	1.783714e-02		ADP ribosylation factor
		PF00071.17	15/71 (21.13%)	4.220867e-02		Ras subfamily
		PF00928.16	5/8 (62.50%)	4.438262e-02		Adaptor complexes medium subunit domain
		PF01399.22	7/17 (41.18%)	4.515427e-02		PCI domain

Table 2: Specific genes with functions related to plant cell wall decay investigated specifically in this study. Both for qRT-PCR analyses, raw count plots of RNAseq and their placement in cluster analyses. For identification, the transcriptome ID from our study (strain FPRL 280) and the JGI protein ID (strain MAD 698-R) is used

Gene (abbreviation)	Transcriptome ID	JGI protein id	Function
Oxalate synthesis and oxalate decomposition			
Glyoxylate dehydrogenase (GlyD)	TRINITY_DN33196_c1_g1	121561	Involved in oxalate synthesis
Oxaloacetate acetylhydrolase (OahA)	TRINITY_DN26529_c1_g1	112832	Involved in oxalate synthesis
Oxalate decarboxylase (OxaD)	TRINITY_DN21938_c3_g2	43912	Involved in oxalate decomposition
Redox enzymes			
AA3 GMC oxidoreductase (AOx1)	TRINITY_DN18773_c0_g1	44331	Involved in oxidative depolymerization. Likely source of H_2O_2.
AA3 GMC oxidoreductases (AOx2)	TRINITY_DN20417_c3_g1	129158	Involved in oxidative depolymerization. Likely source of H_2O_2.
AA3 GMC oxidoreductase (AOx3)	TRINITY_DN28649_c4_g1	118723	Involved in oxidative depolymerization. Likely source of H_2O_2.
AA3_3 Alcohol oxidase (AOx4)	TRINITY_DN21062_c1_g1	55972	Involved in oxidative depolymerization. Likely source of H_2O_2.
AA5 Copper radical oxidase (Cro1)	TRINITY_DN21070_c1_g1	56703	Involved in oxidative depolymerization. Likely source of H_2O_2.
AA5 Copper radical oxidase (Cro2)	TRINITY_DN9270_c1_g1	104114	Involved in oxidative depolymerization. Likely source of H_2O_2.
AA6 Benzoquinone reductases (BqR)	TRINITY_DN21924_c2_g1	124517	Involved in oxidative depolymerization. Possibly involved in reduction/regeneration of chelator/reductants
Cellulose degradation			
GH5 Endoglucanase (Cel5a)	TRINITY_DN26393_c3_g1_i1	115648	Major endocellulase
GH5 Endoglucanase (Cel5b)	TRINITY_DN21725_c8_g1	103675	Major endocellulase
GH12 Glucoside hydrolase (XyGEg)	TRINITY_DN33048_c6_g2	121191	Endoglucanase active on cellulose or xyloglucan
AA9 Lytic polysaccharide monooxygenases (LPMO)	TRINITY_DN16131_c0_g1	126811	Polysaccharide depolymerization via oxidative cleavage of glycosidic bonds.
GH3 Betaglucosidase (bGlu)	TRINITY_DN21749_c2_g1	128500	Hydrolyses cellobiose, releasing glucose
Hemicellulose and pectin degradation			
Endomannanase (Man5a)	TRINITY_DN30802_c4_g1	121831	Involved in glucomannan depolymerization, highly expressed
GH10 Endoxylanase (Xyl10a)	TRINITY_DN11072_c0_g2	113670	Involved in xylose depolymerization
GH10b Endoxylanase (Xyl10b)	TRINITY_DN17151_c1_g1	105534	Involved in xylose depolymerization
GH3 Beta xylosidase (bXyl)	TRINITY_DN28569_c4_g1	51213	Hemicellulose depolymerization
CE16 Carbohydrate esterase (CE16a)	TRINITY_DN26470_c5_g1	125801	Deacetylation of polysaccharides
CE 16 Carbohydrate esterase family 16 (CE16b)	TRINITY_DN21066_c2_g6	48548	Deacetylation of polysaccharides
GH28 Polygalacturonase (Gal28a)	TRINITY_DN7127_c0_g2	111730	Involved pectin depolymerization

Expansins			
Expansin (Exp1)	TRINITY_DN6700_c0_g2	126976	Most likely involved in increasing enzyme accessibility
Expansin (Exp2)	TRINITY_DN24238_c3_g1	128179	Most likely involved in increasing enzyme accessibility

FIGURE LEGENDS

Figure 1. Boxplots of the mass loss of all experiments of *Rhodonia placenta* grown on *Pinus radiata* and different levels of modification by furfurylated *P. radiata*. The weight of the treatment is included the measurements. a) *R. placenta* grown on unmodified P. radiata. Wood harvested at five different harvest points (week). b) *R. placenta* grown on furfurylated *P. radiata*, Weight Percent Gain (WPG) 4%. Wood harvested at three different harvest points. For c) and d) The wood was harvested at six harvest points for *R. placenta* grown on furfurylated *P. radiata*, WPG 23% (c) and WPG 37% (d).

Figure 2. The figures of PCA plots of all the RNAseq replicates of *Rhodonia placenta* grown on *Pinus radiata* and furfurylated *P. radiata*. In total 42% of the variance is explained by the two PCA axis. a) and b) show the same plot, but in a) the replicates are colored according to experiment and in b) the replicates are colored according to harvest time (week).

Figure 3. All genes were clustered into 10 groups according to their similarity in expression patterns based on read counts from RNAseq data. Each treatment was analyzed separately. The figure visualizes the relationship among these gene clusters (tree structure) and their expression pattern related to harvest point (week). Dark color indicates higher expression.

Figure 4. Heatmaps based on dbcan2 annotations of CAZymes suggested to be involved in plant wall decay the mean of all replicates from all experiments of *Rhodonia placenta* grown on *Pinus radiata* and different levels of modification by furfurylated *P. radiata*. Each experiment is plotted separately, with an independent scale. The Gene ID for all transcripts, the dbcan2 annotations and the corresponding gene ID from the qPCR are listed. a) the oxidizing enzymes, b) the core hydrolyzing enzymes, c) the accessory enzymes suggested

to support the core enzymatic apparatus. In the accessory enzyme plot, three genes were removed from the heatmap because of extremely high expression, hiding the signal of the other genes in the *P. radiata* plot. See Fig. S2 for plot over all genes.

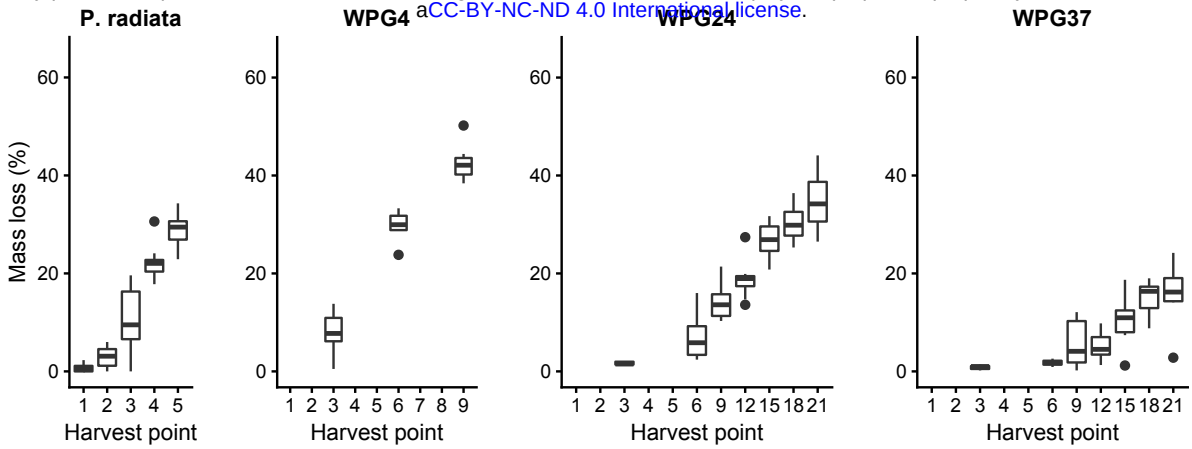

a)

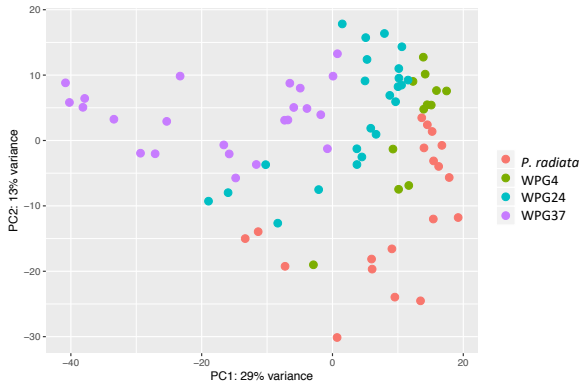

b)

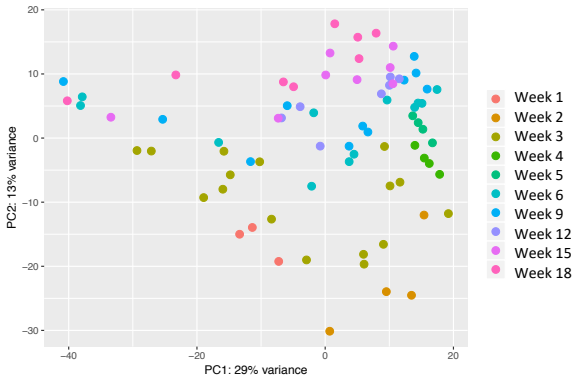

a)

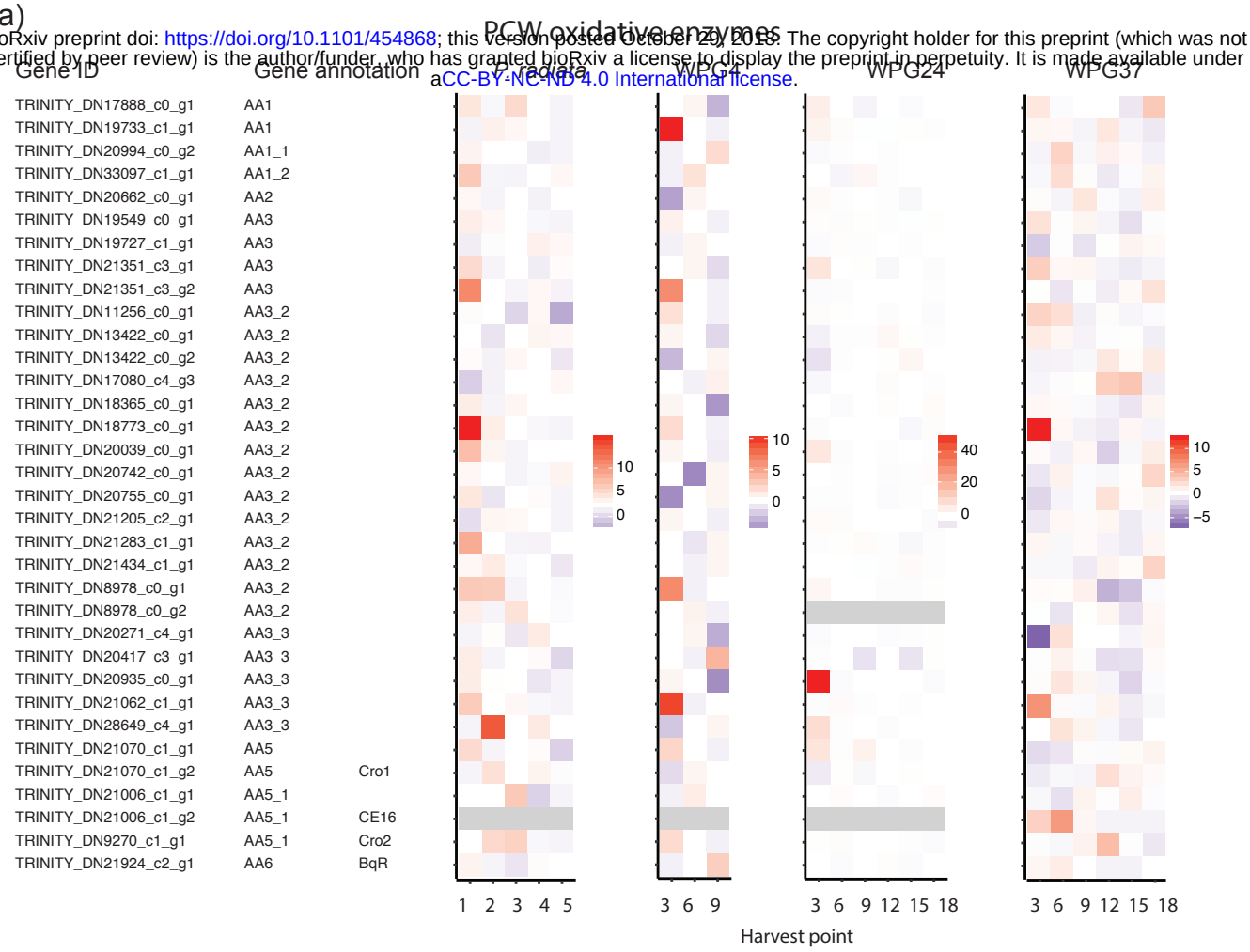

b)

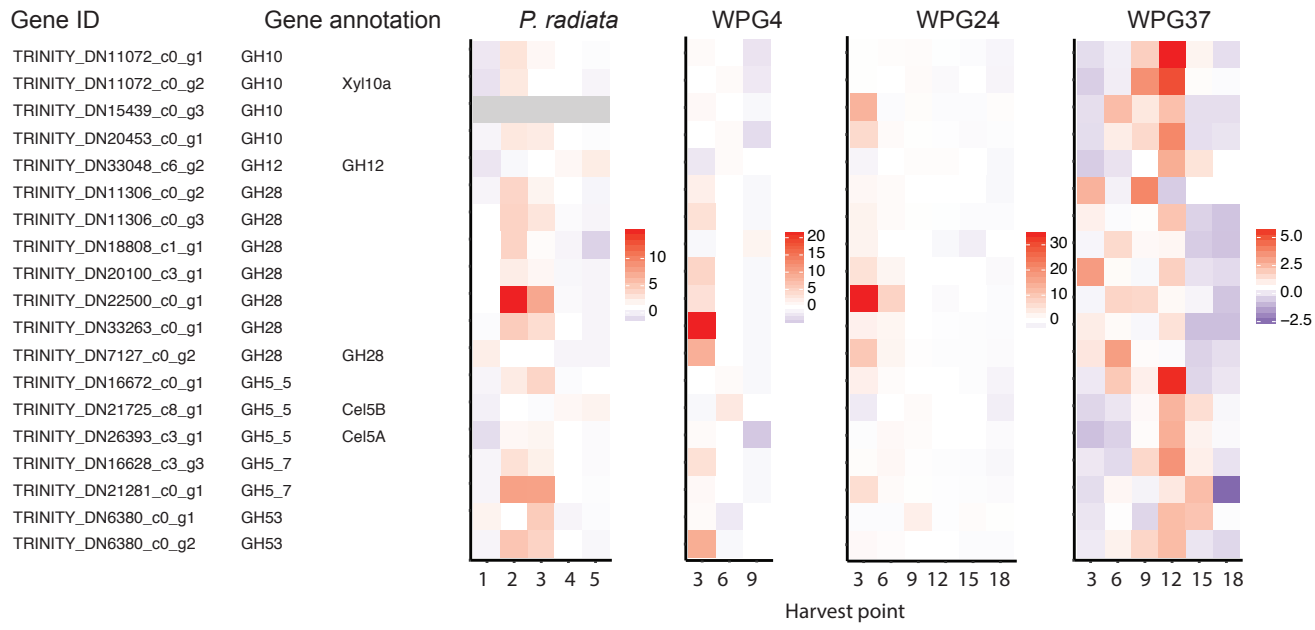

c)